PERSPECTIVE

Interpreting contemporary trends in atmospheric methane

Alexander J. Turner[a,1,2], Christian Frankenberg[b,c,1,2], and Eric A. Kort[d,1,2]

Edited by Mark H. Thiemens, University of California, San Diego, La Jolla, CA, and approved January 9, 2019 (received for review August 18, 2018)

Atmospheric methane plays a major role in controlling climate, yet contemporary methane trends (1982–2017) have defied explanation with numerous, often conflicting, hypotheses proposed in the literature. Specifically, atmospheric observations of methane from 1982 to 2017 have exhibited periods of both increasing concentrations (from 1982 to 2000 and from 2007 to 2017) and stabilization (from 2000 to 2007). Explanations for the increases and stabilization have invoked changes in tropical wetlands, livestock, fossil fuels, biomass burning, and the methane sink. Contradictions in these hypotheses arise because our current observational network cannot unambiguously link recent methane variations to specific sources. This raises some fundamental questions: (*i*) What do we know about sources, sinks, and underlying processes driving observed trends in atmospheric methane? (*ii*) How will global methane respond to changes in anthropogenic emissions? And (*iii*), What future observations could help resolve changes in the methane budget? To address these questions, we discuss potential drivers of atmospheric methane abundances over the last four decades in light of various observational constraints as well as process-based knowledge. While uncertainties in the methane budget exist, they should not detract from the potential of methane emissions mitigation strategies. We show that net-zero cost emission reductions can lead to a declining atmospheric burden, but can take three decades to stabilize. Moving forward, we make recommendations for observations to better constrain contemporary trends in atmospheric methane and to provide mitigation support.

methane trends | greenhouse gas mitigation | tropospheric oxidative capacity

Methane accounts for more than one-quarter of the anthropogenic radiative imbalance since the preindustrial age (1). Its largest sources include both natural and human-mediated pathways: wetlands, fossil fuels (oil/gas and coal), agriculture (livestock and rice cultivation), landfills, and fires (2, 3). The dominant loss of methane is through oxidation in the atmosphere via the hydroxyl radical (OH). Apart from its radiative effects, methane impacts background tropospheric ozone levels, the oxidative capacity of the atmosphere, and stratospheric water vapor. As such, changes in the abundance of atmospheric methane can have profound impacts on the future state of our climate. Understanding the sources and sinks of atmospheric methane is critical to assessing future climate and also global tropospheric background ozone, which can impact air quality.

From ice core records, we know that atmospheric methane levels have nearly tripled since 1800 (4). Blake et al. (5) made the first accurate in situ measurements in 1978 and measurements from the National Oceanic and Atmospheric Administration (NOAA) (6) and Advanced Global Atmospheric Gases Experiment (AGAGE) (7) reached global coverage in 1983. These measurements showed a continued increase (with fluctuations) until ∼2000 when the globally averaged concentration stabilized at 1,750 parts per billion (ppb) (8). In 2007 atmospheric levels began increasing again (9, 10), with this rise continuing today. There has been much speculation about the cause of these recent trends, with numerous seemingly contradictory explanations (2, 3, 8–31). Attribution of these trends has proved to be a difficult task because (*i*) this period of renewed growth is characterized by a source–sink

[a]Department of Earth and Planetary Sciences, University of California, Berkeley, CA 94720; [b]Division of Geological and Planetary Sciences, California Institute of Technology, Pasadena, CA 91226; [c]Jet Propulsion Laboratory, California Institute of Technology, Pasadena, CA 91109; and [d]Climate and Space Sciences and Engineering, University of Michigan, Ann Arbor, MI 48109

Author contributions: A.J.T., C.F., and E.A.K. designed research, performed research, analyzed data, and wrote the paper.

The authors declare no conflict of interest.

This article is a PNAS Direct Submission.

[1]A.J.T., C.F., and E.A.K. contributed equally to this work.

[2]To whom correspondence may be addressed. Email: alexjturner@berkeley.edu, cfranken@caltech.edu, or eakort@umich.edu.

Published online February 7, 2019.

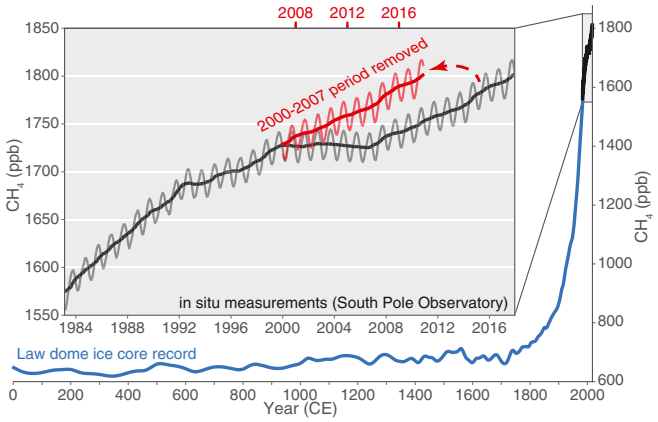

Fig. 1. Observations of atmospheric methane over the past 2,000 y. Shown are Law Dome ice core record (blue) (4) and direct atmospheric observations from the South Pole (black, deseasonalized in gray) (6). Red line illustrates if the 7-y stabilization period is removed.

imbalance of only 3% and (*ii*) there are a myriad of diverse processes with large uncertainties that could potentially emit methane. Here we leverage the extensive work conducted by the methane community over the last decades to clarify the current state of the science, specifically addressing the following: (*i*) What do we know about sources, sinks, and underlying processes driving observed trends in atmospheric methane? (*ii*) How will global methane respond to changes in anthropogenic emissions? And (*iii*), What future observations could help resolve changes in the methane budget?

Recent History of Atmospheric Methane

Preindustrial atmospheric methane levels were stable over the last millenium at ~600–700 ppb, as inferred from ice core measurements in Antarctica (Fig. 1). Methane concentrations have been altered by humans even before industrialization (32) but began increasing more rapidly in the 1900s (4) due to both human agricultural activities and expanded use of fossil fuels. This rapid rise closely mirrors that of other greenhouse gases that are driven by industrialization and agriculture (e.g., CO_2) (1). There is no debate about the cause of the bulk of this rise in atmospheric methane from preindustrial times to the present: human activities.

It is likely that natural sources of methane changed during this period as well; for example, Arora et al. (33) found an increase in simulated wetland emissions from 1850 to 2000 due to changes in temperature and Dean et al. (34) discuss how natural methane emissions may change in response to climatic changes. However, these changes in natural sources are small relative to the more than 300 Tg/y increase in anthropogenic sources from preindustrial times to the present (1, 3, 35). This rise in atmospheric methane from preindustrial levels continued unabated until the 1990s, at which point the methane record diverged from CO_2 and N_2O (which both showed continued growth).

Methane concentrations stabilized in 2000 (8) and then growth resumed in 2007 (9, 10) that continues today (6, 7). This period from 2000 to 2007 is referred to as the "stabilization" and the increase from 2007 to present is referred to as the "renewed growth." Both stabilization and renewed growth have seen conflicting explanations in the literature. Dlugokencky et al. (8) suggested that this stabilization may be a new steady state for atmospheric methane and, as such, many analyses have viewed the period of renewed growth as anomalous. This view of the renewed growth as a departure from steady state has led to a search for methane sources that increased in 2007. However, if the stabilization period is removed from the contemporary methane record, then the long-term trend becomes a continuous rise (Fig. 1, *Inset*) with little change in the growth rate. One may wonder which period (if any) is anomalous in the contemporary methane record: If one expects steady state, then the renewed growth appears anomalous; conversely if one expects a long-term rise, then the stabilization appears anomalous. These two views may result in different research foci. For example, the former view may lead one to search for an increasing source while the latter may lead one to look for a decline in sources or increasing sink. The renewed growth has now continued for more than a decade, underlining that the 7-y stabilization period could be considered as anomalous. This perspective does not necessarily require a new, sustained emissions increase in 2007 as many papers have sought. The gaps that need explanation become the anomalous stabilization period and the evolving combination of emissions that contribute to the continued rise.

Atmospheric Clues and Inventory/Process Understanding of Atmospheric Methane

Explanations of recent atmospheric methane trends can be broadly grouped based on the types of proxy measurements used. Measurements of $\delta^{13}C\text{-}CH_4$ (the $^{13}C/^{12}C$ ratio in atmospheric methane) provide information about the fraction of methane coming from biotic (i.e., microbial) and abiotic sources, as biotic methane is produced enzymatically and tends to be depleted in ^{13}C, making it isotopically lighter. Atmospheric ethane (C_2H_6) can be coemitted with methane from oil/gas activity and, as such, has been used as a tracer for fossil methane emissions (11, 15, 18–20). Similarly, carbon monoxide can be coemitted with methane from biomass burning. Methyl chloroform (CH_3CCl_3) is a banned industrial solvent that has been used to infer the abundance of the dominant methane sink (the hydroxyl radical, OH) (38, 42–46). These four measurements ($\delta^{13}C\text{-}CH_4$, C_2H_6, CO, and CH_3CCl_3) have been used in conjunction with atmospheric methane measurements. However, studies generally reached differing conclusions regarding the recent methane trends.

Fig. 2, *Left* shows the observations of atmospheric methane and the proxies used to explain the stabilization and renewed growth. Studies using ethane have argued that decreases in fossil fuel sources led to the stabilization of atmospheric methane in the 2000s (e.g., refs. 11 and 15) and that increases in fossil fuel sources contributed to the growth since 2007 (e.g., refs. 18–20). Studies using isotope measurements tend to find that decreases in microbial sources led to the stabilization (e.g., ref. 12) and increases in microbial sources are responsible for the renewed growth (e.g., refs. 17, 24, and 25). Studies that include methyl chloroform measurements tend to find that changes in the methane sink played a role in both the stabilization and renewed growth (e.g., refs. 22, 27, 28, and 47). Finally, Worden et al. (31) included measurements of carbon monoxide and inferred a decrease in biomass burning emissions, an isotopically heavy methane source, that helps reconcile a potential increase in both fossil fuel and microbial emissions.

The problem of inferring processes responsible for the stabilization and renewed growth is often underconstrained when framed in a global or hemispherically integrated manner. From a globally integrated perspective, we have three observables (CH_4, $\delta^{13}C\text{-}CH_4$, CH_3CCl_3) and attempt to infer changes in methane emissions, the partitioning between methane source sectors, CH_3CCl_3 emissions, and OH concentrations. Solving this requires additional constraints, which can also have large uncertainties.

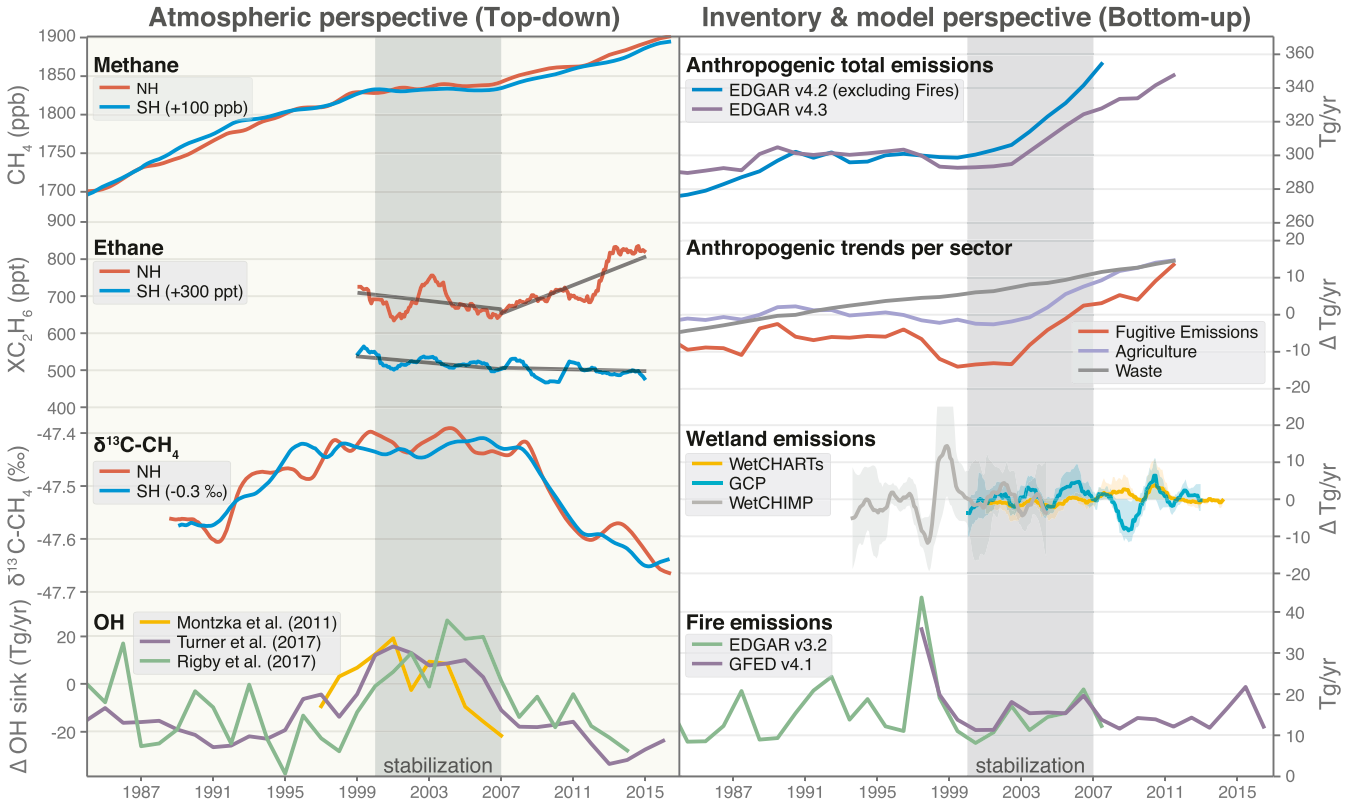

Fig. 2. Constraints on atmospheric methane over the past 40 y. *Left* column illustrates atmospheric constraints: methane (6), ethane (18), δ^{13}C-CH_4 (ftp://aftp.cmdl.noaa.gov/data/ and www.iup.uni-heidelberg.de/institut/forschung/groups/kk/en/) (36, 37), and OH sink inferred from methyl chloroform (27, 28, 38), assuming a global methane source of 550 Tg/y. Black lines in the ethane panel are taken directly from Hausmann et al. (18). *Right* column illustrates deseasonalized process and inventory representations for the same time period: total anthropogenic (35), anthropogenic disaggregated to three most important anthropogenic sectors, wetland models (30, 39, 40), and fire emission estimates (41). The stabilization period is indicated in both columns by the vertical gray area.

Adding ethane or carbon monoxide helps only if we can assume that their emission ratios (CH_4/C_2H_6 or CH_4/CO) and their variation in time are well known and well characterized. Many studies have assumed that OH is unchanging in the atmosphere (e.g., refs. 17, 24, and 25) because it is well buffered (38, 48), thus making the problem well posed, leading to stronger conclusions regarding the processes driving the stabilization and renewed growth. However, changes of a few percent in OH are sufficient to perturb the global budget (27, 28), with a 4% decrease in global mean OH being roughly equivalent to a 22 Tg/y increase in methane emissions.

Fig. 2, *Right* shows our current inventory- and process-based understanding of global methane sources. Based on this, the only sources that show a multidecadal trend are anthropogenic (waste, agriculture, and fugitives from fossil fuels). Natural sources and sinks (e.g., wetlands, fires, and OH) exhibit substantial variability on subdecadal scales but we do not have a process/inventory-based explanation for a long-term trend. For example, Poulter et al. (30) were unable to explain the renewed growth with changes in wetland emissions. Some individual wetland models do find increases in emissions [e.g., McNorton et al. (49)], but the increases are small (2 Tg/y) relative to the source–sink imbalance (20 Tg/y). Variations in many of these natural sources and sinks have been found to be driven in part by the El Niño–Southern Oscillation (ENSO) (e.g., refs. 31 and 50–53). The long-term growth trend in atmospheric methane is best explained by the continued rise in anthropogenic emissions—even though the most uncertain sectors are predominantly natural (wetlands and OH)—and as long as anthropogenic emissions continue to rise we expect a concurrent rise in atmospheric methane with variability superimposed due to fluctuations in natural sources and sinks. There is significant uncertainty in anthropogenic emissions, as evidenced when two different versions of the same inventory produce different expected emissions (Fig. 2, *Top Right*), but anthropogenic sources remain alone as able to explain the long-term rise in methane emissions over the past 40 y.

As mentioned above, there are large uncertainties in many aspects of the methane budget relative to the changes needed to reconcile the contemporary trends. Specifically, a 20 Tg/y imbalance (or ∼3.5% change) in the source–sink budget is sufficient to explain observed changes in methane. Current uncertainties in individual components of the methane budget greatly exceed this threshold. Namely, uncertainties in OH are on the order of 7% [1-σ from Rigby et al. (28), corresponding to ±38 Tg/y]; differences in tropical wetlands can be as large as 80 Tg/y [max–min from Saunois et al. (3)]; and the uncertainties in the δ^{13}C-CH_4 source signatures for fossil fuel and microbial sources are 10.7‰ and 6.2‰, respectively [1-σ from Sherwood et al. (54)], which are large enough to attribute the entire source–sink imbalance to either fossil or nonfossil sources [supplemental section 1 in Turner et al. (27)].

Can all of the various lines of evidence be consistently explained? If we focus on the perspective that the stabilization period is anomalous, it can be identified as a time of elevated OH relative to preceding and succeeding years. This shift alone could explain

the stabilization period as well as the renewed increase. It is likely a decrease in anthropogenic emissions in the late 1990s (masked at first by the large fire emissions from El Niño) also contributed. There has been a long-term decline in atmospheric ethane [Simpson et al. (15)] that can be seen in the Southern Hemispheric ethane record in Fig. 2; however, the Northern Hemispheric measurements have been more variable and Hausmann et al. (18) suggest an increase since 2007 due to an increase in fossil fuel emissions. Inventories also predict increased fossil fuel emissions, but estimated resumption starting a few years earlier, in the middle of the stabilization period. While there may be a timing offset in the inventory, the more recent increase in atmospheric ethane could also be largely driven by expanded production of gas in wet oil fields where C_2H_6:CH_4 ratios are very large (55). These proposed source/sink changes would require concomitant changes in the partitioning between isotopically heavy and light sources to satisfy the constraints from δ^{13}C-CH_4. It is tempting to conclude the isotopic shift in atmospheric methane must prove the growth is driven by an increase in microbial emissions; however, the problem is underconstrained in a globally integrated framework and one can find scenarios that are consistent with the δ^{13}C-CH_4 measurements that include increasing fugitive fossil fuel emissions [e.g., Worden et al. (31)].

All studies that include measurements of methyl chloroform find changes in OH that resemble those shown in Fig. 2, *Bottom Left* (e.g., refs. 22, 27, 28, 38, and 47) while studies that do not include methyl chloroform find that changes in sources alone drive contemporary trends and that OH changes are negligible (e.g., refs. 17, 24, and 56). This implies that either (*i*) there are latent issues in how methyl chloroform observations are being used to estimate OH or (*ii*) future work on methane trends should include measurements of methyl chloroform to jointly infer OH. Studies that attributed methane trends to OH (e.g., refs. 22, 27, and 28) did not identify a physical mechanism for the OH changes and the lack of a mechanism remains a valid criticism (e.g., ref. 57). Holmes et al. (58) discuss the processes that impact global mean OH (and methane lifetime) and found temperature, water vapor, stratospheric ozone column, biomass burning, lightning NO_x, and methane abundance to be important drivers. Gaubert et al. (59) found that decreases in CO emissions may have increased OH from 2002 to 2013, opposite to what has been inferred via methyl chloroform. Recently, Turner et al. (52) found ENSO to be the dominant mode of OH variability in the absence of external forcing, acting primarily through changes in deep convection and lightning NO_x. However, as mentioned above, ENSO would likely contribute to the variability but not long-term trends.

Further, papers that inferred OH changes from the available observational constraints (e.g., refs. 27 and 28) did not explicitly simulate the feedbacks with CH_4 or CO as suggested by Prather and Holmes (60). In summary, we currently lack independent evidence to confirm or refute OH changes. At the same time, we need to consider that mechanistic global atmospheric chemistry transport models fail to even simulate the partitioning of OH between the Northern and Southern Hemispheres (e.g., refs. 44 and 61), which alone warrants further OH studies. It should also be stressed that a similar discrepancy between what mechanistic models predict and what is inferred from observations holds for wetlands, where an ensemble of wetland models is inconsistent with the hypothesis of a large shift in tropical emissions [Poulter et al. (30) and wetland emissions in Fig. 2, *Right*]. This stresses the need to reconcile process-based models with observations because findings of either large changes in OH or wetland emissions are not particularly enlightening if we fail to understand the causes of these variations.

Isotopic and ethane observations provide valuable clues to the relative balance of sources and sinks of methane. One of the most critical gaps in isotopic- and/or ethane-based global observations is the underlying assumption that source/sink signatures and their variation in time are well known. That is, we a priori know the isotopic (ethane) characteristic of every source (sink) and how it varies in time. However, this assumption generally does not hold. For example, a recent update to our understanding of isotopic characteristics of sources from Sherwood et al. (54) shifted the expected recent historical balance of biotic/abiotic emissions (25, 54). However, this new inventory still has little information on tropical wetlands' microbial signature (only ∼50 samples from tropical wetlands). A further update to the inventory would likely shift the interpretation of the trends and budget. Furthermore, the assumption of temporally invariant signatures is likely false, as the δ^{13}C-CH_4 signal from a wetland is the balance of production (methanogenesis) and loss (oxidation by methanotrophs)—if that wetland exhibits changing fluxes in response to changing water/temperature, the relative production/loss terms will shift and the isotopic signal will change (e.g., refs. 62 and 63). McCalley et al. (64) demonstrated this for microbial communities in permafrost thaw and Dean et al. (34) highlighted the importance of quantifying whether consumption by microbes will balance production in the future. A similar problem holds for ethane, where oil/gas fields have drastically different C_2:C_1 ratios, and within a single field this ratio can change over the history of production of a field. In addition, different amounts of ethane are extracted from natural gas, depending on the economic value of ethane as petrochemical feedstock. These confounding factors are more tractable at higher spatial resolution (e.g., the isotopic source signatures and C_2:C_1 ratios are well characterized for individual sources or basins) than at the global or hemispheric scale.

Spatial gradients in observed methane concentration have also been used to infer emissions at a variety of scales. This is typically done via "atmospheric inversions," using models to account for atmospheric transport. Houweling et al. (65) provide an extensive review of work on atmospheric inversions over the past 25 years that was started by Fung et al. (66) in 1991. Briefly, these atmospheric inversions have leveraged existing surface, aircraft, and satellite observations to infer our best understanding of methane fluxes for specific time frames (e.g., refs. 51 and 67–79). The Global Carbon Project (GCP) published a synthesis of the methane budget in 2013 [Kirschke et al. (2)] that was recently updated by Saunois et al. (3) based on an ensemble of inversions. The GCP highlighted the importance of reducing the uncertainty on wetland emissions and reducing "double counting" of sources. It did not address changes in the methane sink but reported a climatological range for the sink based primarily on the work of Naik et al. (61). Atmospheric inversions are limited by the spatiotemporal coverage of the observations and our ability to accurately simulate atmospheric transport. As such, increases in the spatiotemporal coverage of traceable, calibrated, and validated observations (from surface, aircraft, or satellite) and improvements in atmospheric transport models would help this approach in constraining the methane budget.

Space-borne observations of methane and proxies related to specific sectors represent an attractive constraint on the methane budget [e.g., Sellers et al. (80)], as they provide a unique

spatial coverage. Jacob et al. (81) provide a detailed review of the role of satellite observations. Briefly, satellite observations have proved to be be useful in constraining methane sources at local-to-regional scales (e.g., refs. 16, 74, 75, 77, 78, and 82–84) but have thus far played a relatively limited role in the discussion of global methane trends because the record is short compared with in situ measurements. For example, the first total column measurements of methane were made by Scanning Imaging Absorption Spectrometer for Atmospheric Chartography (SCIAMACHY) in 2003 (73, 85) and Greenhouse Gases Observing Satellite (GOSAT) (86) is the longest-running satellite that measures total column methane with 9 y of data (measurements started in April 2009) (87, 88). Networks like the Total Carbon Column Observing Network (TCCON) (89) and AirCore [Karion et al. (90)] are crucial to identify biases in satellite measurements, evaluate their uncertainties, and facilitate intercomparisons between different satellite instruments. Satellite observations will likely play a growing role in the discussion of future methane trends as the record length increases and new missions like the recently launched Tropospheric Monitoring Instrument (TROPOMI) (91) and recently funded Geostationary Carbon Cycle Observatory (GeoCARB) instrument (geostationary orbit) (92) emerge. TROPOMI launched in October 2017 and reported encouraging observations of CO (93) and methane (94). For satellites to provide their full potential value added, rigorous validation and traceability are necessary. Atmospheric inversions should also attempt to cope with potential biases in satellite data by jointly inferring bias terms.

The role of specific regions such as the United States and the Arctic in recent methane trends is also debated. For example, Turner et al. (16) inferred an increase in US emissions but Bruhwiler et al. (95) find that this increase is inconsistent with a model ensemble from the GCP. This topic (US methane emissions) was the focus of a review paper by Miller and Michalak (96) and a recent National Academy of Sciences Report (97); however, the role of US methane emissions is still under debate [Sheng et al. (98)]. It underlines the sobering fact that even for the data-rich United States, we still cannot conclusively determine whether there has been a long-term trend in methane emissions. The role of methane emissions from the East Siberian Arctic Shelf (ESAS) is another topic that has been heavily debated in the recent literature. Work from Shakhova et al. (99) extrapolated ship-based measurements to estimate ESAS methane emissions; however, more recent work from Berchet et al. (100), Thornton et al. (101), and Warwick et al. (102) found emissions that were a factor of 4–30 lower. Widespread emissions of methane hydrates are unlikely [Ruppel et al. (103)] as methane sources in waters deeper than 100 m have negligible contributions to the atmosphere (104, 105) and recent work from Sparrow et al. (106) uses radiocarbon measurements from the Beaufort Shelf in the Arctic Ocean to infer that less than 10% of methane in surface water is from sources deeper than 30 m. More broadly, there has been a lot of interest in understanding how methane emissions from the Arctic may change in the future because of the temperature dependence of microbial methane sources and enhanced warming due to Arctic amplification (1). While it is important to understand these regional emissions, current uncertainties in the tropics greatly exceed the absolute magnitude of Arctic sources. Further, Sweeney et al. (107) suggest Arctic emission changes would have little impact on global budgets if the temperature sensitivity is similar to what has been observed in the present. This is not to discount the potential importance of future Arctic methane emissions, but the prime uncertainties in the current global methane budget lie in the tropics for a number of reasons: (*i*) tropical wetlands are the largest natural source, (*ii*) methane oxidation through OH is largest in the tropics, and (*iii*) the ground-based observational network is least dense and frequent cloud cover reduces satellite data densities.

Impact of Changing Anthropogenic Methane Emissions on Global Methane

Despite the uncertainty of the current relative balance of different controls on atmospheric methane, there is no debate that the large increase from preindustrial times is driven by anthropogenic emissions and that reducing anthropogenic emissions can lead to direct, near-term decreases in atmospheric methane. However, changing methane emissions will alter the methane lifetime via chemical feedbacks with OH [Prather (108, 109)] and, as such, atmospheric abundances can exhibit longer timescales than one may assume. We illustrate this in Fig. 3 by using a simple box model [adapted from Turner et al. (27)] to evaluate four scenarios to bound the future methane abundances: continued growth in anthropogenic methane emissions (case A), a stabilization of methane emissions in 2012 (case B), and an emission decrease over 10 y (case C) or instantaneously (case D). The emissions decrease in the latter two scenarios is based on a recent report from the International Energy Agency (110) that estimates current methane emissions from oil and gas could be reduced by 40–50% with zero net cost. For all scenarios, we consider how these changes in methane abundances will impact OH using a simplified CH_4-CO-OH system [Prather (108, 109)] and cases where methane does not feed back on OH. The latter case with constant OH is meant to account for factors that might buffer methane-induced OH changes [e.g., changes in the ozone photolysis rate or changes in NO_x emissions; see Murray et al. (111) and Holmes et al. (58) for a discussion of some of these factors]. The methane emissions and OH anomalies for these four scenarios are shown in Fig. 3, *Left* and *Right*, respectively.

In Fig. 3, *Center* we see the range of possible methane responses. With increasing emissions, atmospheric levels increase unabated. Important subtleties remain: If OH dynamically responds to methane, atmospheric levels would be 180 ppb higher in the case of continued increasing emissions. Even if emissions stabilized in 2012, atmospheric levels are still increasing in 2050 with interactive OH. This highlights a subtle but important point relevant for understanding recent atmospheric methane behavior: with emissions stabilization atmospheric methane can still increase for more than three decades [see Prather (108, 109) for a detailed discussion of these feedbacks and their relation to the eigenvalues of the chemical system]. In the scenarios of net-zero cost emission reductions, we do see the atmosphere exhibits decreases in atmospheric concentrations, but depending on the time frame of emission reductions, the atmospheric decrease can take a decade to detect it, and if OH responds dynamically, atmospheric abundances of methane will remain significantly higher (~50 ppb). Also worth noting, in all of the dynamic OH cases a significant perturbation is projected. In the case of continued rising emissions, this could impact global mean OH by ~10%—a large shift that could have profound impacts on the oxidative capacity of the global atmosphere (e.g., ref. 112).

How Can We Do Better Moving Forward?

Long-term in situ observations provide the backbone upon which our current understanding of atmospheric methane is founded. Continuation of these observations is paramount to observing and

understanding future methane changes. However, it is now abundantly clear that these in situ observations alone are not sufficient for unequivocally partitioning contemporary variations in atmospheric methane (from 1980 to the present) to specific source/sink pathways. This is, in part, because contemporary methane trends are driven by a source–sink imbalance of ∼20 Tg/y (or ∼3.5%) yet uncertainties in regional and sectoral components of the methane budget greatly exceed this threshold. In particular, methane emissions from wetlands have an uncertainty of ∼40 Tg/y [range from Saunois et al. (3) is 80 Tg/y] and methane loss due to reaction with OH has an uncertainty of ∼7% [or ±38 Tg/y; e.g., Rigby et al. (28)]. These two sectors represent the largest sources of uncertainty in the methane budget and reconciling the contemporary trends will require observations that can (*i*) provide better constraints on these uncertain sectors and (*ii*) improve our process-level understanding and representation at regional scales. Expansion of the current observational network of methane (and coemitted species) from surface or space will provide valuable information. However, no single program is likely to settle the debate; addressing the major uncertainties in the contemporary methane budget will require a concerted effort in multiple areas. Here we highlight a few potential pathways toward better constraining future methane emissions and their drivers.

i) Expand Measurement Networks to Include More Proxies for Methane Source Partitioning. Radiocarbon (^{14}C; e.g., ref. 113), deuterium (i.e., δD), and "clumped" isotopologue measurements (molecules multiply substituted with rarer isotopes, such as $^{13}CH_3D$ or $^{12}CH_2D_2$; ref. 114) could provide additional leverage on partitioning the global budget because they would help isolate changes due to the most uncertain sectors (e.g., wetlands and OH). Specifically, radiocarbon measurements would help to separate fossil and nonfossil methane emissions [Petrenko et al. (113)] while clumped isotopologue measurements can constrain biogenic/thermogenic emissions [Stolper et al. (114)] or the loss via reaction with OH [Haghnegahdar et al. (115)]. However, both of these measurements will require advances in the analytical techniques before they could be used in ambient conditions. δD measurements, on the other hand, are less useful than radiocarbon or clumped isotopologues but the measurements are substantially easier to make. All of these isotopic measurements could help to constrain the most uncertain sectors in the methane budget, but there is a trade-off between added value and cost. Expanded studies of source signatures would be required for these isotope-driven approaches to provide maximum value. Radiocarbon shows potential with a less extensive source signature study requirement, as this tracer provides a cleaner delineation between fossil and contemporary methane sources. We encourage more observing-system simulation studies that quantify the added values of different proxies as well as redundancies, at the local to regional and global scales. In the interim, archiving of air samples [such as those at Commonwealth Scientific and Industrial Research Organisation (CSIRO), ref. 116] would provide an affordable strategic approach for enabling future measurements of attributive tracers that are infeasible with current technology or have not yet been recognized. As such, expansion of the air archive would enable the community to work backward in future years and address the most uncertain aspects of the methane budget.

ii) Targeted Measurement and Modeling Programs Focused on Tropical Wetlands and Global OH. These sectors are currently the largest uncertainties in interpreting trends in methane and moving forward will continue to present a challenge unless we can improve the observational constraints and our ability to represent emissions/uptake with process-driven models. Development of high-resolution inventories that resolve, for example, wetland and lake emissions without double counting [e.g., Thornton et al. (117)] and spatially resolved isotopic source signatures [e.g., Ganesan et al. (118)] will be crucial to help reduce uncertainties in the use of isotopologue measurements. Dense observations (ground, airborne or space-borne, campaign or sustained) coupled with methane wetland model development for multiple tropical regions could provide a pathway toward more accurate representation and understanding of emissions from this sector. A similar observational approach was applied to the US oil and gas sector [Alvarez et al. (119)] that led to substantial improvements in the representation of methane sources [Zavala-Araiza et al. (120)]. Such a campaign could help improve the dynamics

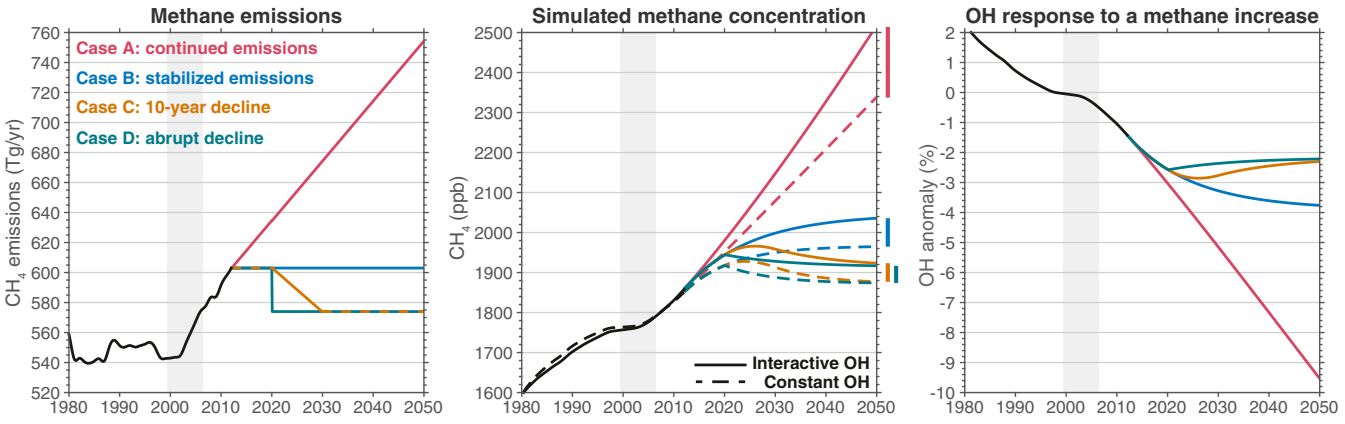

Fig. 3. Projections of atmospheric methane over the next 30 y. (*Left*) The methane emissions from 1980 to 2050 under four different emission scenarios: continued growth in anthropogenic emissions (case A, red), stabilization of emissions in 2012 (case B, blue), and an emission decrease over 10 y (case C, orange) or instantaneously (case D, green). Anthropogenic emissions from 1980 to 2012 are from Emission Database for Global Atmospheric Research (EDGAR) v4.3 (black). (*Center*) The simulated methane concentrations under the four emission scenarios with interactive OH (solid line) and a constant OH concentration (dashed line; no OH or CO feedback). Colored vertical lines to the right of the panel show the range of the CH_4 concentrations in 2050 for interactive and constant OH. (*Right*) The OH anomaly due to changes in methane and CO. The stabilization period in all panels is indicated by the vertical gray shading.

of methane emissions in wetland models (including regionally relevant isotopic source signatures) and their sensitivity to changes in temperature and inundation. Global OH presents a different challenge, as point measurements of OH are unlikely to adequately sample the variability in OH to the precision needed for methane trends (better than 3%). Further, the methyl chloroform constraints on OH are degrading with time as the ambient concentrations of methyl chloroform are now ∼2 parts per trillion (a 50-fold decrease from the 1990s) (27); alternate strategies need to be developed [Liang et al. (46)]. Recent work from Zhang et al. (53) suggests that satellite observations of midtropospheric methane could be used for this purpose. Additional work using existing measurements, such as those from AirCore [Karion et al. (90)] or the Atmospheric Tomography Experiment (ATom) (https://espo.nasa.gov/atom/content/ATom), and future campaigns should further investigate the possibility of inferring OH with midtropospheric measurements from satellites.

Implications for Emissions Mitigation

While uncertainties in the methane budget exist, they should not detract from the key points discussed here. Namely, reducing anthropogenic methane emissions will slow or reverse the rise in atmospheric concentrations; however, depending on the timescale and magnitude of reduction, it may take decades before atmospheric levels decline. When considering recent decades, the stabilization period is emerging as anomalous due in part to fluctuations in natural sources/sinks, whereas the last decade of growth continues the long-term, increasing trend that is due to human activities.

Even with present uncertainties on global methane trends, there have been a a number of recent advances in measurement technology that have tremendous potential for opportunistic mitigation (i.e., reducing emissions at no net cost). A few notable examples include identifying large fugitive leaks in oil and gas infrastructure and changing the diet of livestock. Specifically, remote sensing has demonstrated the ability to identify anomalous, large emitters and focused programs to use aircraft- or space-based observations to identify and mitigate emissions could prove cost efficient and effective (82, 121–125). Recent advances in frequency-comb spectrometers (126, 127) and affordable, small ground-based sensors may also provide a mitigation opportunity for superemitters in oil/gas basins (128). Changes in the diet of livestock could reduce the production of methane in dairy cattle without reducing milk production and, as such, could be an opportunity to reduce methane emissions from livestock (129, 130). Implementation of these or other mitigation strategies could help to curb future increases in atmospheric methane and provide detectable changes in the global methane burden within decades.

Acknowledgments

We thank the Linde Center for Global Environmental Science at California Institute of Technology for supporting the workshop that made this study possible. We are extremely grateful to the many participants in said workshop ("Toward Addressing Major Gaps in the Global Methane Budget"; workshop.caltech.edu/methane/): A. A. Bloom, P. Bousquet, L. M. Bruhwiler, G. Chadwick, P. Crill, G. Etiope, S. Houweling, D. J. Jacob, F. Keppler, J. D. Maasakkers, C. Miller, S. Naus, E. Nisbet, M. Okumua, B. Poulter, M. Prather, J. Randerson, K. M. Saad, S. Sander, D. Schimel, C. Sweeney, K. Verhulst, D. Wunch, and Y. Yin. The insights and conversations from this group improved this study. Finally, this work would not have been possible without the tireless efforts and public data sharing of scientists making long-term measurements, pursuing atmospheric modeling, and developing inventories: specifically, the NOAA/Earth Systems Research Lab (ESRL) Global Greenhouse Gas Reference Network and AGAGE for CH_4; R. Sussmann and D. Smale for XC_2H_6; NOAA/Institute of Arctic and Alpine Research (INSTARR), University of California, Irvine, University of Washington, and University of Heidelberg for $\delta^{13}C\text{-}CH_4$; A. A. Bloom for the Wetland Methane Emissions and Uncertainty (WetCHARTs) inventory; B. Poulter for the GCP wetlands; and J. R. Melton for The Wetland and Wetland CH_4 Inter-comparison of Models Project (WetCHIMP). A.J.T. is supported as a Miller Fellow with the Miller Institute for Basic Research in Science at University of California, Berkeley.

1 IPCC (2013) Climate change 2013: The physical science basis. *Contribution of Working Group I to the Fifth Assessment Report of the Intergovernmental Panel on Climate Change*, (*IPCC*, Cambridge Univ Press, New York), Technical Report.
2 Kirschke S, et al. (2013) Three decades of global methane sources and sinks. *Nat Geosci* 6:813–823.
3 Saunois M, et al. (2016) The global methane budget 2000–2012. *Earth Syst Sci Data* 8:697–751.
4 Etheridge DM, Steele LP, Francey RJ, Langenfelds RL (1998) Atmospheric methane between 1000 A.D. and present: Evidence of anthropogenic emissions and climatic variability. *J Geophys Res* 103:15979–15993.
5 Blake DR, et al. (1982) Global increase in atmospheric methane concentrations between 1978 and 1980. *Geophys Res Lett* 9:477–480.
6 Dlugokencky E (2018) Trends in atmospheric methane. Available at NOAA/ESRL (www.esrl.noaa.gov/gmd/ccgg/trends_ch4/). Accessed November 12, 2018.
7 Prinn R, Weiss RF (2018) Advanced global atmospheric gases experiment. Available at AGAGE (https://agage.mit.edu/). Accessed November 12, 2018.
8 Dlugokencky EJ, et al. (2003) Atmospheric methane levels off: Temporary pause or a new steady-state? *Geophys Res Lett* 30:1992.
9 Rigby M, et al. (2008) Renewed growth of atmospheric methane. *Geophys Res Lett* 35:L22805.
10 Dlugokencky EJ, et al. (2009) Observational constraints on recent increases in the atmospheric CH_4 burden. *Geophys Res Lett* 36:L18803.
11 Aydin M, et al. (2011) Recent decreases in fossil-fuel emissions of ethane and methane derived from firn air. *Nature* 476:198–201.
12 Kai FM, Tyler SC, Randerson JT, Blake DR (2011) Reduced methane growth rate explained by decreased Northern Hemisphere microbial sources. *Nature* 476:194–197.
13 Bousquet P, et al. (2011) Source attribution of the changes in atmospheric methane for 2006–2008. *Atmos Chem Phys* 11:3689–3700.
14 Levin I, et al. (2012) No inter-hemispheric $\delta^{13}CH_4$ trend observed. *Nature* 486:E3–E4.
15 Simpson IJ, et al. (2012) Long-term decline of global atmospheric ethane concentrations and implications for methane. *Nature* 488:490–494.
16 Turner AJ, et al. (2016) A large increase in U.S. methane emissions over the past decade inferred from satellite data and surface observations. *Geophys Res Lett* 43:2218–2224.
17 Schaefer H, et al. (2016) A 21st-century shift from fossil-fuel to biogenic methane emissions indicated by $^{13}CH_4$. *Science* 352:80–84.
18 Hausmann P, Sussmann R, Smale D (2016) Contribution of oil and natural gas production to renewed increase in atmospheric methane (2007–2014): Top-down estimate from ethane and methane column observations. *Atmos Chem Phys* 16:3227–3244.
19 Franco B, et al. (2016) Evaluating ethane and methane emissions associated with the development of oil and natural gas extraction in North America. *Environ Res Lett* 11:044010.
20 Helmig D, et al. (2016) Reversal of global atmospheric ethane and propane trends largely due to US oil and natural gas production. *Nat Geosci* 9:490–495.
21 Dalsøren SB, et al. (2016) Atmospheric methane evolution the last 40 years. *Atmos Chem Phys* 16:3099–3126.
22 McNorton J, et al. (2016) Role of OH variability in the stalling of the global atmospheric CH_4 growth rate from 1999 to 2006. *Atmos Chem Phys* 16:7943–7956.
23 Rice AL, et al. (2016) Atmospheric methane isotopic record favors fossil sources flat in 1980s and 1990s with recent increase. *Proc Natl Acad Sci USA* 113:10791–10796.
24 Nisbet EG, et al. (2016) Rising atmospheric methane: 2007-2014 growth and isotopic shift. *Glob Biogeochem Cy* 30:1356–1370.

25 Schwietzke S, et al. (2016) Upward revision of global fossil fuel methane emissions based on isotope database. *Nature* 538:88–91.
26 Saunois M, et al. (2017) Variability and quasi-decadal changes in the methane budget over the period 2000–2012. *Atmos Chem Phys* 17:11135–11161.
27 Turner AJ, Frankenberg C, Wennberg PO, Jacob DJ (2017) Ambiguity in the causes for decadal trends in atmospheric methane and hydroxyl. *Proc Natl Acad Sci USA* 114:5367–5372.
28 Rigby M, et al. (2017) Role of atmospheric oxidation in recent methane growth. *Proc Natl Acad Sci USA* 114:5373–5377.
29 Bader W, et al. (2017) The recent increase of atmospheric methane from 10 years of ground-based NDACC FTIR observations since 2005. *Atmos Chem Phys* 17:2255–2277.
30 Poulter B, et al. (2017) Global wetland contribution to 2000–2012 atmospheric methane growth rate dynamics. *Environ Res Lett* 12:094013.
31 Worden JR, et al. (2017) Reduced biomass burning emissions reconcile conflicting estimates of the post-2006 atmospheric methane budget. *Nat Commun* 8:2227.
32 Ruddiman WF (2013) The anthropocene. *Annu Rev Earth Planet Sci* 41:45–68.
33 Arora VK, Melton JR, Plummer D (2018) An assessment of natural methane fluxes simulated by the CLASS-CTEM model. *Biogeosciences* 15:4683–4709.
34 Dean JF, et al. (2018) Methane feedbacks to the global climate system in a warmer world. *Rev Geophys* 56:207–250.
35 European Commission (2013) Global emissions EDGAR v4.2 FT2010. Available at edgar.jrc.ec.europa.eu/overview.php?v=42FT2010. Accessed November 12, 2018.
36 Carbon Dioxide Information Analysis Center (2012) Measurements of atmospheric methane and $^{13}C/^{12}C$ of atmospheric methane from flask air samples. Available at https://cdiac.ess-dive.lbl.gov/ndps/quay.html. Accessed November 12, 2018.
37 Carbon Dioxide Information Analysis Center (2004) Mixing ratios of CO, CO_2, CH_4, and isotope ratios of associated ^{13}C, ^{18}O, and ^{2}H in air samples from Niwot Ridge, Colorado, and Montaña de Oro, California, USA. Available at https://cdiac.ess-dive.lbl.gov/epubs/db/db1022/db1022.html. Accessed November 12, 2018.
38 Montzka SA, et al. (2011) Small interannual variability of global atmospheric hydroxyl. *Science* 331:67–69.
39 Bloom AA, et al. (2017) A global wetland methane emissions and uncertainty dataset for atmospheric chemical transport models (WetCHARTs version 1.0). *Geosci Mod Dev* 10:2141–2156.
40 Melton JR, et al. (2013) Present state of global wetland extent and wetland methane modelling: Conclusions from a model inter-comparison project (WETCHIMP). *Biogeosciences* 10:753–788.
41 van der Werf GR, et al. (2010) Global fire emissions and the contribution of deforestation, savanna, forest, agricultural, and peat fires (1997–2009). *Atmos Chem Phys* 10:11707–11735.
42 Spivakovsky CM, et al. (2000) Three-dimensional climatological distribution of tropospheric OH: Update and evaluation. *J Geophys Res* 105:8931–8980.
43 Prinn RG, et al. (2001) Evidence for substantial variations of atmospheric hydroxyl radicals in the past two decades. *Science* 292:1882–1888.
44 Prather MJ, Holmes CD, Hsu J (2012) Reactive greenhouse gas scenarios: Systematic exploration of uncertainties and the role of atmospheric chemistry. *Geophys Res Lett* 39:L09803.
45 Patra PK, et al. (2014) Observational evidence for interhemispheric hydroxyl-radical parity. *Nature* 513:219–223.
46 Liang Q, et al. (2017) Deriving global OH abundance and atmospheric lifetimes for long-lived gases: A search for CH_3CCl_3 alternatives. *J Geophys Res* 122:11914–11933.
47 McNorton J, et al. (2018) Attribution of recent increases in atmospheric methane through 3-D inverse modelling. *Atmos Chem Phys* 18:18149–18168.
48 Lelieveld J, Gromov S, Pozzer A, Taraborrelli D (2016) Global tropospheric hydroxyl distribution, budget and reactivity. *Atmos Chem Phys* 16:12477–12493.
49 McNorton J, et al. (2016) Role of regional wetland emissions in atmospheric methane variability. *Geophys Res Lett* 43:11433–11444.
50 Bousquet P, et al. (2006) Contribution of anthropogenic and natural sources to atmospheric methane variability. *Nature* 443:439–443.
51 Zhu Q, et al. (2017) Interannual variation in methane emissions from tropical wetlands triggered by repeated El Nino Southern oscillation. *Glob Change Biol* 23:4706–4716.
52 Turner AJ, Fung I, Naik V, Horowitz LW, Cohen RC (2018) Modulation of hydroxyl variability by ENSO in the absence of external forcing. *Proc Natl Acad Sci USA* 115:8931–8936.
53 Zhang Z, et al. (2018) Enhanced response of global wetland methane emissions to the 2015–2016 El Niño-Southern oscillation event. *Environ Res Lett* 13:074009.
54 Sherwood OA, Schwietzke S, Arling VA, Etiope G (2017) Global inventory of gas geochemistry data from fossil fuel, microbial and burning sources, version 2017. *Earth Syst Sci Data* 9:639–656.
55 Kort EA, et al. (2016) Fugitive emissions from the Bakken shale illustrate role of shale production in global ethane shift. *Geophys Res Lett* 43:4617–4623.
56 Thompson RL, et al. (2018) Variability in atmospheric methane from fossil fuel and microbial sources over the last three decades. *Geophys Res Lett* 45:11499–11508.
57 Brownlow R, et al. (2017) Isotopic ratios of tropical methane emissions by atmospheric measurement. *Glob Biogeochem Cy* 31:1408–1419.
58 Holmes CD, Prather MJ, Sovde OA, Myhre G (2013) Future methane, hydroxyl, and their uncertainties: Key climate and emission parameters for future predictions. *Atmos Chem Phys* 13:285–302.
59 Gaubert B, et al. (2017) Chemical feedback from decreasing carbon monoxide emissions. *Geophys Res Lett* 44:9985–9995.
60 Prather MJ, Holmes CD (2017) Overexplaining or underexplaining methane's role in climate change. *Proc Natl Acad Sci USA* 114:5324–5326.
61 Naik V, et al. (2013) Preindustrial to present-day changes in tropospheric hydroxyl radical and methane lifetime from the Atmospheric Chemistry and Climate Model Intercomparison Project (ACCMIP). *Atmos Chem Phys* 13:5277–5298.
62 Conrad R, et al. (2011) Stable carbon isotope discrimination and microbiology of methane formation in tropical anoxic lake sediments. *Biogeosciences* 8:795–814.
63 Whiticar MJ (1999) Carbon and hydrogen isotope systematics of bacterial formation and oxidation of methane. *Chem Geol* 161:291–314.
64 McCalley CK, et al. (2014) Methane dynamics regulated by microbial community response to permafrost thaw. *Nature* 514:478–481.
65 Houweling S, et al. (2017) Global inverse modeling of CH_4 sources and sinks: An overview of methods. *Atmos Chem Phys* 17:235–256.
66 Fung I, et al. (1991) Three-dimensional model synthesis of the global methane cycle. *J Geophys Res* 96:13033.
67 Hein R, Crutzen PJ, Heimann M (1997) An inverse modeling approach to investigate the global atmospheric methane cycle. *Glob Biogeochem Cy* 11:43–76.
68 Bergamaschi P, et al. (2007) Satellite chartography of atmospheric methane from SCIAMACHY on board ENVISAT: 2. Evaluation based on inverse model simulations. *J Geophys Res* 112:D02304.
69 Houweling S, van der Werf GR, Klein Goldewijk K, Rockmann T, Aben I (2008) Early anthropogenic CH_4 emissions and the variation of CH_4 and $^{13}CH_4$ over the last millennium. *Glob Biogeochem Cy* 22:GB1002.
70 Bergamaschi P, et al. (2009) Inverse modeling of global and regional CH_4 emissions using SCIAMACHY satellite retrievals. *J Geophys Res* 114:D22301.
71 Meirink JF, Bergamaschi P, Krol MC (2008) Four-dimensional variational data assimilation for inverse modelling of atmospheric methane emissions: Method and comparison with synthesis inversion. *Atmos Chem Phys* 8:6341–6353.
72 Miller SM, et al. (2013) Anthropogenic emissions of methane in the United States. *Proc Natl Acad Sci USA* 110:20018–20022.
73 Bergamaschi P, et al. (2013) Atmospheric CH_4 in the first decade of the 21st century: Inverse modeling analysis using SCIAMACHY satellite retrievals and NOAA surface measurements. *J Geophys Res* 118:7350–7369.
74 Fraser A, et al. (2013) Estimating regional methane surface fluxes: The relative importance of surface and GOSAT mole fraction measurements. *Atmos Chem Phys* 13:5697–5713.
75 Cressot C, et al. (2014) On the consistency between global and regional methane emissions inferred from SCIAMACHY, TANSO-FTS, IASI and surface measurements. *Atmos Chem Phys* 14:577–592.
76 Wecht KJ, et al. (2014) Spatially resolving methane emissions in California: Constraints from the CalNex aircraft campaign and from present (GOSAT, TES) and future (TROPOMI, geostationary) satellite observations. *Atmos Chem Phys* 14:8173–8184.
77 Turner AJ, et al. (2015) Estimating global and North American methane emissions with high spatial resolution using GOSAT satellite data. *Atmos Chem Phys* 15:7049–7069.

78 Alexe M, et al. (2015) Inverse modelling of CH_4 emissions for 2010–2011 using different satellite retrieval products from GOSAT and SCIAMACHY. *Atmos Chem Phys* 15:113–133.
79 Houweling S, et al. (2014) A multi-year methane inversion using SCIAMACHY, accounting for systematic errors using TCCON measurements. *Atmos Chem Phys* 14:3991–4012.
80 Sellers PJ, Schimel DS, Moore B, Liu J, Eldering A (2018) Observing carbon cycle–climate feedbacks from space. *Proc Natl Acad Sci USA* 115:7860–7868.
81 Jacob DJ, et al. (2016) Satellite observations of atmospheric methane and their value for quantifying methane emissions. *Atmos Chem Phys* 16:14371–14396.
82 Kort EA, et al. (2014) Four corners: The largest US methane anomaly viewed from space. *Geophys Res Lett* 41:6898–6903.
83 Wecht KJ, Jacob DJ, Frankenberg C, Jiang Z, Blake DR (2014) Mapping of North American methane emissions with high spatial resolution by inversion of SCIAMACHY satellite data. *J Geophys Res* 119:7741–7756.
84 Ganesan AL, et al. (2017) Atmospheric observations show accurate reporting and little growth in India's methane emissions. *Nat Comm* 8:836.
85 Frankenberg C, Meirink JF, van Weele M, Platt U, Wagner T (2005) Assessing methane emissions from global space-borne observations. *Science* 308:1010–1014.
86 Kuze A, et al. (2016) Update on GOSAT TANSO-FTS performance, operations, and data products after more than 6 years in space. *Atmos Meas Tech* 9:2445–2461.
87 Butz A, et al. (2011) Toward accurate CO_2 and CH_4 observations from GOSAT. *Geophys Res Lett* 38:L14812.
88 Parker R, et al. (2011) Methane observations from the greenhouse gases observing SATellite: Comparison to ground-based TCCON data and model calculations. *Geophys Res Lett* 38:L15807.
89 Wunch D, et al. (2011) The total carbon column observing network. *Philos Trans R Soc A* 369:2087–2112.
90 Karion A, Sweeney C, Tans P, Newberger T (2010) AirCore: An innovative atmospheric sampling system. *J Atmos Ocean Tech* 27:1839–1853.
91 Butz A, et al. (2012) TROPOMI aboard Sentinel-5 precursor: Prospective performance of CH_4 retrievals for aerosol and cirrus loaded atmospheres. *Proc SPIE* 120:267–276.
92 Polonsky IN, O'Brien DM, Kumer JB, O'Dell CW (2014) Performance of a geostationary mission, geoCARB, to measure CO_2, CH_4 and CO column-averaged concentrations. *Atmos Meas Tech* 7:959–981.
93 Borsdorff T, et al. (2018) Measuring carbon monoxide with TROPOMI: First results and a comparison with ECMWF-IFS analysis data. *Geophys Res Lett* 45:2826–2832.
94 Hu H, et al. (2018) Toward global mapping of methane with TROPOMI: First results and intersatellite comparison to GOSAT. *Geophys Res Lett* 45:3682–3689.
95 Bruhwiler LM, et al. (2017) U.S. CH_4 emissions from oil and gas production: Have recent large increases been detected? *J Geophys Res* 122:4070–4083.
96 Miller SM, Michalak AM (2017) Constraining sector-specific CO_2 and CH_4 emissions in the US. *Atmos Chem Phys* 17:3963–3985.
97 National Academy of Sciences (2018) *Improving Characterization of Anthropogenic Methane Emissions in the United States* (National Academies of Sciences, Washington, DC).
98 Sheng JX, et al. (2018) 2010–2016 methane trends over Canada, the United States, and Mexico observed by the GOSAT satellite: Contributions from different source sectors. *Atmos Chem Phys* 18:12257–12267.
99 Shakhova N, et al. (2013) Ebullition and storm-induced methane release from the East Siberian arctic shelf. *Nat Geosci* 7:64–70.
100 Berchet A, et al. (2016) Atmospheric constraints on the methane emissions from the East Siberian shelf. *Atmos Chem Phys* 16:4147–4157.
101 Thornton BF, Geibel MC, Crill PM, Humborg C, Morth CM (2016) Methane fluxes from the sea to the atmosphere across the Siberian shelf seas. *Geophys Res Lett* 43:5869–5877.
102 Warwick NJ, et al. (2016) Using. δ^{13}C-CH_4 and δD-CH_4 to constrain Arctic methane emissions. *Atmos Chem Phys* 16:14891–14908.
103 Ruppel CD, Kessler JD (2017) The interaction of climate change and methane hydrates. *Rev Geophys* 55:126–168.
104 McGinnis DF, Greinert J, Artemov Y, Beaubien SE, Wuest A (2006) Fate of rising methane bubbles in stratified waters: How much methane reaches the atmosphere? *J Geophys Res* 111:C09007.
105 Pohlman JW, et al. (2017) Enhanced CO_2 uptake at a shallow Arctic ocean seep field overwhelms the positive warming potential of emitted methane. *Proc Natl Acad Sci USA* 114:5355–5360.
106 Sparrow KJ, et al. (2018) Limited contribution of ancient methane to surface waters of the U.S. Beaufort sea shelf. *Sci Adv* 4:eaao4842.
107 Sweeney C, et al. (2016) No significant increase in long-term CH_4 emissions on North Slope of Alaska despite significant increase in air temperature. *Geophys Res Lett* 43:6604–6611.
108 Prather MJ (1994) Lifetimes and eigenstates in atmospheric chemistry. *Geophys Res Lett* 21:801–804.
109 Prather MJ (2007) Lifetimes and time scales in atmospheric chemistry. *Philos Trans R Soc A* 365:1705–1726.
110 International Energy Agency (2017) *World Energy Outlook 2017* (IEA Publications, Paris).
111 Murray LT, et al. (2014) Factors controlling variability in the oxidative capacity of the troposphere since the last glacial maximum. *Atmos Chem Phys* 14:3589–3622.
112 Shindell D, et al. (2012) Simultaneously mitigating near-term climate change and improving human health and food security. *Science* 335:183–189.
113 Petrenko VV, et al. (2017) Minimal geological methane emissions during the Younger Dryas-Preboreal abrupt warming event. *Nature* 548:443–446.
114 Stolper DA, et al. (2014) Gas formation. Formation temperatures of thermogenic and biogenic methane. *Science* 344:1500–1503.
115 Haghnegahdar MA, Schauble EA, Young ED (2017) A model for $^{12}CH_2D_2$ and $^{13}CH_3D$ as complementary tracers for the budget of atmospheric CH_4. *Glob Biogeochem Cy* 31:1387–1407.
116 Krummel P, John Gorman J, Downey A (2018) Cape grim air archive. Available at CSIRO (https://researchdata.ands.org.au/cape-grim-air-archive). Accessed November 12, 2018.
117 Thornton BF, Wik M, Crill PM (2016) Double-counting challenges the accuracy of high-latitude methane inventories. *Geophys Res Lett* 43:12569–12577.
118 Ganesan AL, et al. (2018) Spatially resolved isotopic source signatures of wetland methane emissions. *Geophys Res Lett* 45:3737–3745.
119 Alvarez RA, et al. (2018) Assessment of methane emissions from the U.S. oil and gas supply chain. *Science* 361:186–188.
120 Zavala-Araiza D, et al. (2015) Reconciling divergent estimates of oil and gas methane emissions. *Proc Natl Acad Sci USA* 112:15597–15602.
121 Thompson DR, et al. (2015) Real-time remote detection and measurement for airborne imaging spectroscopy: A case study with methane. *Atmos Meas Tech* 8:4383–4397.
122 Frankenberg C, et al. (2016) Airborne methane remote measurements reveal heavy-tail flux distribution in Four Corners region. *Proc Natl Acad Sci USA* 113:9734–9739.
123 Conley S, et al. (2016) Methane emissions from the 2015 Aliso Canyon blowout in Los Angeles, CA. *Science* 351:1317–1320.
124 Turner AJ, et al. (2018) Assessing the capability of different satellite observing configurations to resolve the distribution of methane emissions at kilometer scales. *Atmos Chem Phys* 18:8265–8278.
125 Varon DJ, et al. (2018) Quantifying methane point sources from fine-scale satellite observations of atmospheric methane plumes. *Atmos Meas Tech* 11:5673–5686.
126 Rieker GB, et al. (2014) Frequency-comb-based remote sensing of greenhouse gases over kilometer air paths. *Optica* 1:290.
127 Coburn S, et al. (2018) Regional trace-gas source attribution using a field-deployed dual frequency comb spectrometer. *Optica* 5:320.
128 Cusworth DH, et al. (2018) Detecting high-emitting methane sources in oil/gas fields using satellite observations. *Atmos Chem Phys* 2018:1–25.
129 Hristov AN, et al. (2015) An inhibitor persistently decreased enteric methane emission from dairy cows with no negative effect on milk production. *Proc Natl Acad Sci USA* 112:10663–10668.
130 Niu M, et al. (2018) Prediction of enteric methane production, yield, and intensity in dairy cattle using an intercontinental database. *Glob Change Biol* 24:3368–3389.